HHS Public Access

Author manuscript

Expert Rev Ophthalmol. Author manuscript; available in PMC 2024 November 01.

Published in final edited form as:

Expert Rev Ophthalmol. 2023 ; 18(6): 379–389. doi:10.1080/17469899.2023.2277781.

Principles of Ophthalmic Ultrasound

Ronald H. Silverman[1]

[1]Columbia Irving Medical Center, New York, NY, United States

Abstract

Introduction: Ultrasound imaging of the eye was introduced over 50 years ago. While the physical principles of ultrasound imaging have not changed, technology has undergone tremendous and ongoing development.

Areas covered: The fundamentals of ultrasound physics, biometry (A-scan), structural imaging (B-scan) and blood-flow imaging and measurement (Doppler) will be described. Emphasis will be placed on technological development and potential future advances.

Expert opinion: While A- and B-scan ultrasound of the eye has traditionally been performed with focused single-element transducers, the introduction of annular and linear arrays has enhanced clinical utility. Future advances, especially in multielement arrays, and point-of-care systems promise amazing new capabilities for diagnostic imaging of the eye and orbit.

Keywords

ultrasound; eye; Doppler; transducer

1. Introduction

As with many other modern technologies, medical diagnostic ultrasound was born of war. During the First World War, there was a desperate need to detect enemy submarines due to unrestricted U-boat attacks on shipping in the North Atlantic. Paul Langevin worked on an acoustic solution to this problem for the French government during the war, but this technology, later called SONAR (from “sound navigation ranging”), was not ready before the war was over. SONAR, however, was widely used by all sides during the Second World War. Medical diagnostic ultrasound systems were developed from this technologic foundation in the war’s aftermath.

Both SONAR and medical ultrasound are based on the same principles:

- Echoes will be produced when a sound wave encounters an interface differing in acoustic impedance (density × speed-of-sound) from the surrounding medium.

Corresponding author: Ronald H. Silverman, Department of Ophthalmology, Columbia University Irving Medical Center, 701 West 168th Street, Room 609B, New York, NY 10032, rs3072@cumc.columbia.edu.

Declaration of interest

R H Silverman has a financial interest in Arcscan, Inc. The author has no other relevant affiliations or financial involvement with any organization or entity with a financial interest in or financial conflict with the subject matter or materials discussed in the manuscript apart from those disclosed.

- The range to the reflecting interface can be computed from time-of-flight between transmission of an acoustic pulse and echo reception if the speed of sound in the medium is known.
- By controlling the direction of the acoustic pulse and measuring time-of-flight, the position of the reflector can be estimated.

2. Physics and Engineering Principles

Ultrasound is simply sound above the frequency range of human hearing, i.e., <20,000 cycles/sec (20 kHz), but medical ultrasound systems use frequencies in the millions of cycles/sec (MHz) range. Like sound, ultrasound is a mechanical disturbance characterized by compression and rarefaction that propagates as a longitudinal wave at a characteristic speed in a fluid medium or biologic tissue. The speed of ultrasound is independent of frequency. When the wave encounters an acoustic impedance discontinuity, partial reflection will occur. Ultrasound imaging is based on detection of such reflections.

The components of an ultrasound system include a transducer for converting voltage transients to ultrasound pulses, a pulser for electrical excitation of the transducer, a receiver for amplifying minute voltages produced at the transducer by echoes, a mechanism for scanning, and a display device.

A piezoelectric material incorporated in the transducer converts a voltage transient (a spike or monocycle) to an ultrasound wave. The piezoelectric element is typically backed by a material to damp vibrations so that short pulses suitable for imaging are produced.

If the speed of sound in a medium is known, then the range of reflecting interface from the transducer can be determined by measuring the time from pulse transmission to echo return, $r = ct/2$, where r is range, c is the speed of sound and t is time from transmit to echo reception. Images can be generated if we record both range and direction to each echo source.

The waveform of the pulse transmitted by the transducer can equivalently be characterized in the ‘time domain’ as pressure variation over time, or in the ‘frequency domain’ as acoustic power as a function of frequency. Transducers are said to have a *nominal* frequency, e.g., 10 MHz, but actually emit over a bell-shaped frequency band centered about this frequency. The ‘bandwidth’ of the transmitted spectrum is inversely related to pulse length. Bandwidth is expressed as a percentage, specifically the full-width half-maximum frequency range with respect to the center frequency. These concepts are illustrated in Figure 1.

Axial resolution is the ability to discern between two reflectors along the beam’s path. For ultrasound, axial resolution is defined as one half of pulse length. Since the minimum possible pulse length is a wavelength (λ), and $\lambda = c/\nu$ (where c = speed of sound and ν = frequency), it is apparent that axial resolution improves as frequency increases. Pulse length, however, is determined not only by frequency but also the number of cycles per pulse. Therefore, a poorly damped (narrowband) high frequency transducer may not provide better axial resolution than a highly damped (broadband) lower frequency transducer.

Narrowband probes tend to offer good sensitivity, but reduced resolution.[1] They also produce greater speckle, an artifactual granular appearance of tissue caused by interference between overlapping echoes from numerous randomly distributed unresolved scatterers within a tissue resolution volume.

Lateral resolution is the ability to discern between two points perpendicular to the ultrasound beam axis. A flat, unfocused transducer does not in general provide useful lateral resolution. It produces a beam narrowing with depth in its near field (or Fresnel zone), beyond which the beam diverges with depth in its far field (or Fraunhofer zone). The near/far field transition occurs at a distance $A^2/4\lambda$ from the transducer, where A represents aperture. By using a very small aperture, nearfield beamwidth (and lateral resolution) is comparable to aperture, but the near/far field transition distance is small as well. For instance, the transition distance for a 10 MHz transducer with 0.5 mm aperture, is ~0.4 mm, whereas for a 3 mm aperture, it is ~15 mm. So, while an unfocused transducer can produce good lateral resolution if the aperture is tiny, this is only true for a small distance from the probe.

High lateral resolution can be achieved by focusing. Focusing can be implemented either by fabricating a curved piezoelectric element or by superimposing an acoustic lens over a flat element. Focal beamwidth is computed as $F\lambda$, where F is the transducer F-number, i.e., focal length/aperture. For example, a 10 MHz transducer (λ=150 μm) with a 5-mm aperture and 20-mm focal length would have a 0.6 mm focal beamwidth.

A related concept is *temporal resolution*, meaning the number of images that can be produced per second. This is significant in obviating motion artifacts and visualizing tissue motions, especially blood flow, which will be described below in greater detail.

While ultrasound is a propagating pressure wave rather than an electromagnetic wave as is light, both are subject to Snell's law, which describes refraction across an interface between media having different propagation speeds. Also, like light, when ultrasound encounters an interface, the wave is reflected at an angle equal to the angle of incidence. For this reason, the sonographer orients the probe as normally as possible to the tissue under evaluation. This is particularly important when imaging specular surfaces such as the cornea or a lens implant.

At normal incidence, the amplitude of the reflection with respect to that of the incident pulse is $A_i(Z_2 - Z_1)/(Z_1 + Z_2)$, where A_i is the amplitude of the incident pulse and Z_1 and Z_2 represent the acoustic impedances of the media on either side of their interface. Note that because of the large impedance differences between the transducer itself, the air and biologic tissue which result in near-total reflection, ultrasound cannot effectively be used without an acoustic coupling agent, such as gel, between the probe and tissue.

Ultrasound is attenuated as it propagates due to absorption and scattering. Attenuation increases exponentially as frequency increases. At very high frequencies, even water attenuates sufficiently to limit imaging depth. While tissues differ significantly in their attenuation coefficients, a 'rule of thumb' for soft tissues is an attenuation of approximately 0.5 dB/cm-MHz.

Echoes from reflectors moving towards or away from the transducer are frequency shifted with respect to the spectrum of the transmitted pulse because the reflected waveform is compressed or stretched. This is the well-known Doppler effect. By measuring frequency shift, it is possible to depict regions of blood flow and measure flow velocity.

3. Ultrasound imaging and biometry of the eye

All research studies conducted by the author followed the tenets of the Declaration of Helsinki and were approved by the Institutional Review Board.

3.1 A- and B-scan development

A-scan ("Amplitude scan") refers to plotting echo amplitude as a function of range along one line-of-sight. By scanning the transducer to sweep out a plane, a two-dimensional image can be produced by setting pixel brightness proportional to echo amplitude at appropriate ranges and orientations. B-scan ("Brightness scan") refers to this two-dimensional structural imaging.

In ophthalmology, the first A-scan systems were developed by Oksala[2] and B-scans by Baum and Greenwood[3,4] in the 1950's. Oksala, Jansson and Begui and their coworkers made crucial contributions by measuring the speed of sound in ocular media.[5–7] This was of great significance given the contemporaneous introduction of phacoemulsification by Kelman [8] and biocompatible implantable intraocular lenses (IOLs) by Sir Harold Ridley. (Ridley, a British ophthalmologist, had noticed that fragments of shattered acrylic World War II fighter canopies were well-tolerated in eyes [9] - another example of war-derived advancements.) With known speeds-of-sound in the ocular media, axial length could be accurately determined prior to cataract surgery and an appropriate lens power determined. [10] Prior to this, IOL powering was based solely on presurgical refractive error which often resulted in large post-operative refractive errors.

3.1 A-scan systems

Clinical applications: Axial length determination for intraocular lens implant power determination; intraocular tumor thickness and tissue characterization, corneal thickness measurement

Biometric A-scan systems typically operate at 10–15 MHz. The probe includes a central aperture to provide a fixation light to enable alignment of the ultrasound beam axis with the optical axis. A-scan probes may be coupled to the topically anesthetized eye by contact with the central cornea or by use of a fluid standoff, typically provided by a scleral shell. While the contact method can with care produce comparable results to immersion[11], the latter is generally preferred as it obviates potential corneal compression and underestimation of axial length.[12]

Modern A-scan systems will automatically record multiple scans that provide an A-scan pattern consistent with alignment to the optic axis, will assign appropriate speed of sound values to the anterior chamber, lens (normal, cataract, dense cataract, pseudophakic or aphakic), and the vitreous. After removing any outliers, the mean axial length, along with

keratometry K-value, will then be used to recommend intraocular lens power based on one or more formulae, e.g., Holladay[13], Hoffer[14], SRK/T[15], to name a few.

Ultrasound axial length determination has to a great extent been superseded by laser interferometry systems such as the IOLMaster (Zeiss, Jena, Germany) because of their precision and non-contact exam. Nevertheless, ultrasound A-scan is still utilized, especially when dense cataract or other optical opacities are present.

Ultrasound pachymetry is an A-scan technique for measurement of corneal thickness in which a high frequency probe is placed in contact with the topically anesthetized cornea. As with axial length determination, a variety of optical techniques are now available for measuring central corneal thickness.[16–18] Although handheld ultrasound pachymetry has some user-dependence and requires topical anesthesia, it remains widely used because of its effectiveness, low cost and convenience.

3.2 B-scan systems

Clinical applications: Visualization of retinal and choroidal detachment; posterior vitreous detachment; vitreous hemorrhage; mass lesions; optic nerve (drusen, papilledema, nerve sheath diameter measurement) and orbit (muscles, fat); real-time assessment of saccade-induced vitreous motions; vitreoretinal traction; foreign body visualization; ‘no view’ due to corneal scar, cataract, hemorrhage

While A-scan offers a plot of reflection amplitude along a single line-of-sight, B-scan provides two-dimensional anatomic images. In 1969, Coleman et al. described a system in which the transducer was pivoted by hand to sweep out a sector and dwell on one line of sight for an overlapping A-scan while coupled to the patient’s eye with a normal saline waterbath.[19,20] While pivoting the probe by hand, an optical encoder triggered pulse excitation at small angular intervals and echo data acquired using analog circuitry. A- and B-scans were displayed on an oscilloscope and recorded with a polaroid camera. (The author used this system, shown in Figure 2, in the 1980’s!)

A more user-friendly system with a sealed handheld, motorized probe was contemporaneously developed by Bronson.[21] This utilized a 7.5 MHz transducer in a water-filled probe sealed with a thin mylar membrane. The probe was pivoted to produce a sector-shaped image and displayed on a black-and-white television monitor. B-scans could be performed by coupling the probe to the eye with gel, through the eyelid or, after topical anesthesia, directly on the conjunctiva. This system proved to be the grandfather of most current ophthalmic B-scan systems.

Until quite recently, most B-scan systems operated at around 10 MHz, which provided good overall quality in imaging the vitreous, retina and orbit. Technologic advances were gradual, mainly centering of development of permanently sealed probes, digital displays, and digital storage of individual images and cineloops (consisting of recordings of several seconds of real-time display). B-scan probes of 20–25 MHz for high resolution imaging of the retina and anterior segment were introduced.

Examples of A- and B-scans produced on a modern instrument (Absolu, Quantel Medical, Cournon-d'Auvergne, France) are provided in Figure 3.

3.3 Ultrasound biomicroscopy

Clinical applications: Visualization of anterior segment (cornea, anterior and posterior chambers, iris, ciliary body, lens, zonules) and anterior vitreous; intraocular lens displacement; glaucoma (narrow or closed angle, plateau iris, iridotomy patency, shunt tubes); hypotony (ciliary body effusion, dialysis clefts); mass lesions and cysts of iris, ciliary body conjunctive and eyelid

Ultrasound biomicroscopy (UBM) is a B-scan technology utilizing high-frequency (≥35 MHz) probes for imaging the anterior segment. High frequency probes were developed by Sherar and Foster [22,23] in the late 1980's and subsequently demonstrated for imaging the anterior segment by Pavlin.[24] The first commercial system (the UBM 840) was developed by Zeiss-Humphrey (San Leandro, CA) in the mid-1990's and later distributed through Paradigm Instruments. The UBM probe moved the transducer in a linear reciprocating motion over a 5 mm range. The probe was quite heavy and supported a few millimeters above the eye by an articulated arm. Because the cap on a sealed probe would introduce unacceptable levels of attenuation, the transducer was exposed and coupled to the eye with a waterbath.

Modern UBM probes are lightweight and may scan either linearly or in a sector geometry. While a scleral shell can be used, disposable water-filled ClearScan membranes are a convenient and effective way to couple the UBM probe to the eye. Modern UBM systems provide a lateral range sufficient to image the anterior segment from angle-to-angle and depth sufficient to measure anterior chamber depth and lens thickness.

A special adaptation of UBM for imaging the cornea is the arc scan. Because the cornea is a specular reflector, scanning with a sector or linear motion only allows imaging of the central cornea. In order to image the full cornea, Coleman, Reinstein, Silverman and their coworkers developed a prototype [25,26], subsequently commercialized by Ultralink, LLC as the Artemis system, to scan the cornea in an arc that approximately matching the cornea's curvature so that the transducer focus would maintain normal incidence with respect to the corneal surface. This system allowed high-resolution imaging and biometry of the full cornea, and by acquiring data along multiple meridians, allowed mapping and *en face* display of the thickness of the epithelium, stroma, and full corneal thickness. Epithelial thickness mapping was proved invaluable in detection of keratoconus[27–29] and corneal response to refractive surgical procedures such as LASIK[30–32]. This technology was further developed and is currently manufactured as the Insight-100 (Arcscan, Inc., Golden, CO). The Insight couples the eye to the probe with a fluid-filled eyecup and performs programmed scan protocols for cornea and anterior segment. An example of anterior segment scans from this system is shown in Figure 4.

3.4 Ultrasound versus OCT

As with the biometric A-scan, OCT has to large extent replaced ultrasound for evaluation of the retina and anterior segment. As stated above, OCT is advantageous in providing a non-contact exam with significantly higher resolution than ultrasound. As optical scattering results from variation in refractive index, OCT images are qualitatively similar in appearance to ultrasound, where scattering results from variation in acoustic impedance. Current OCT systems provide an axial resolution of around 5–10 μm[33] compared to ~150 μm for a 10 MHz B-scan or ~30 μm for UBM. Also, optical scanning is far more rapid than the mechanical transducer motion used in ophthalmic ultrasound systems. While ophthalmic ultrasound systems may provide 10–20 B-scans/sec, OCT systems are capable of >100,000 A-scans/sec. This high frame rate facilitated the development of OCT-angiography (OCTA) systems which can detect and depict regions in the retina where decorrelation between successive scans of each plane indicative of blood flow are demarcated.

Despite its advantages, OCT is limited because of its susceptibility to optical opacities. To image the retina, OCT must pass through the pupil and the vitreous. Imaging depth is up to 3 mm [34], but not penetrating beyond the choroidoscleral junction even with enhancements such as in spectral domain enhanced depth[35] and swept source[36] OCT systems. The presence of optically opaque tissues (iris, sclera) and pathologies (pigmented tumors, cataract, corneal scars) limits the capacity of OCT to image occult structures. In contrast, ultrasound can readily image through optically opaque tissues, including the eyelid. This is also helpful in observing saccade-induced vitreous motions. At the lower end of the frequency range, ultrasound can visualize orbital tissues out to the orbital chiasm.

Anterior segment OCT is also more affected by corneal refraction than is ultrasound; in the cornea the optical refractive index (ratio of speed of light in vacuum versus tissue) of light is 1.34 compared to the refractive index of ultrasound (ratio of speed of sound in normal saline versus tissue) which is approximately 1.05. This makes OCT anterior segment biometry and imaging more susceptible to refraction-induced distortion than ultrasound.[37] OCT is also more susceptible to shadowing of the iridocorneal angle by the sclera than is ultrasound, which sometimes impedes OCT imaging and measurement of angle width. Retroiridal structures including the ciliary body are not or are poorly visualized, which is a distinct disadvantage in assessing glaucoma etiology.

Another important difference between OCT and ultrasound is the level of technical skill required to perform the exam. OCT primarily requires knowledgeable management of the instrument to perform the required exam protocol which is defined in the instrument software. With the exception of the Arcscan Insight, exams are conducted with handheld probes which requires development of eye-hand-eye coordination and the ability to mentally construct a three-dimensional image of ocular anatomy from real-time two-dimensional B-scans. This requires knowledge of ocular anatomy and pathologies and can only be learned from experience.

Table 1 provides a summary of ultrasound and OCT modes, wavelength and imaging rates.

3.5 Ultrasound versus computed tomography (CT) and magnetic resonance imaging (MRI) of the eye

While ultrasound imaging is based on reflection of sound waves, CT is based on absorption of X-radiation. CT's chief advantage over ultrasound is its capacity to produce high-resolution 3D depictions of the eye and orbit. CT images offer high contrast of bone, calcifications and foreign bodies, making it especially valuable in assessing orbital trauma, especially wall fractures.[38] While CT offers high sensitivity to the presence of calcifications in retinoblastoma, the use of ionizing radiation in a pediatric population is discouraged.[39] The adult crystalline lens is also at risk for cataract from ionizing radiation.[40] Another disadvantage is the relatively low contrast among soft tissues, although this can be improved by contrast-enhancement using intravenous iodinated contrast agents.[41]

MRI also offers 3D imaging of the eye and orbit, but without ionizing radiation and with superior soft tissue contrast. MRI excels in imaging the extraocular muscles, and orbital soft tissues, including fat, fibrous connective tissues, the optic nerve, and mass lesions.

In MRI, the body is exposed to a strong magnetic field to which protons, which have a tiny magnetic field produced by their spin, align. The instrument then emits a radiofrequency (RF) pulse that perturbs the aligned protons, and when the RF field is removed, the protons realign (relax) and lose energy by emitting an RF signal that is detected by the instrument. The most common MRI sequences are T1-weighted and T2-weighted scans which enhance the signal from fatty tissue and water respectively.[42] While clinical MRIs typically use 1.5 or 3T field strength, recently developed 7T systems offer improved signal-to-noise and contrast. [43,44]

Both MRI and CT are disadvantageous with respect to ultrasound in being unavailable at the point of care in a real-time exam. The disadvantages of MRI include the long acquisition time, which can result in motion artifacts and reduced resolution. The potential presence of metallic foreign bodies that could interact with the magnetic field is of course contraindicated. MRI, however, is less operator dependent than ultrasound and is not limited by the perpendicular orientation constraint of ultrasound for imaging the optic nerve and other tissues.[45]

4. Technologic advances

4.1 Annular arrays:

Mechanically scanned, focused single-element probes have long been and remain the staple of ophthalmic ultrasound since Bronson's pioneering system in the 1970's. The reader should, however, be made aware that this is highly atypical of medical ultrasound overall, where array-based systems predominate.

The simplest array-based probe is the annular array. This is quite similar to the single-element systems described above, but instead of one focused piezoelectric element, the element is divided into a series of concentric rings (annuli) that can independently transmit and receive. Ketterling and Silverman described prototype annular arrays for ophthalmic imaging nearly two decades ago.[46,47] Today, manufacturers are offering 20 MHz annular

array probes for ophthalmic imaging. The advantage of the annular array over single-element probes is that by careful timing of annuli excitation, the focal length can be varied electronically to place the focus in mid-vitreous or on the retina. By rapidly transmitting at a series of focal lengths, it is possible to combine the echo data to form an image with an extended depth of field. Compared to linear array systems (described below), annular arrays are simple, comprised of just a few (5 or 6) annuli. The disadvantage of the annular array is that, as in single element systems, it must be scanned mechanically. An example of annular array images is provided in Figure 5.

4.2 Linear arrays:

In linear arrays, on the order of 100 individual transducer elements are arranged, as the name suggests, in a line. The elements are spaced one wavelength or less apart to avoid artifacts that would degrade image quality. Thus, a 10 MHz array ($\lambda \approx 150$ μm) with 100 elements would have a 15 mm aperture. During imaging, groups of adjacent elements function as a subaperture. By careful timing of the excitation of the elements of the subaperture, a converging, focused, wavefront is formed. As with the annular array, the focal length can be varied electronically. Echo data can be similarly beamformed (dynamic focusing).[48] By iterating this process from one side of the array to the other, a rectangular B-mode image is formed. Although linear arrays typically have adequate aperture to capture the full eye width, curvilinear arrays and phased arrays can produce the familiar sector geometry.

Since there is no mechanical motion during scanning with these systems, the scan rate is limited only by the time from pulse transmission to echo reception. For the eye, this is roughly 50 μsec, so for a 100-element array, a B-scan can be acquired in about 5 msec, for a 200 frames/sec scan rate.

This high speed facilitates Doppler ultrasound methods that allow visualization and measurement of blood flow that cannot be performed using mechanically scanned systems. Color flow Doppler displays a red and blue color overlay (respectively indicating flow towards or away from the transducer) upon the greyscale B-scan indicative of axial flow velocity and direction. Power Doppler displays Doppler amplitude. Color flow Doppler is useful for distinguishing arterial from venous flow, while power Doppler is more sensitive and is unaffected by aliasing (an artifactual change in blood flow direction in high-velocity areas) and scan angle.

Accurate measurement of flow velocities requires a pulse rate such that aliasing is avoided. For pulsed Doppler, the required pulse repetition frequency (PRF) is $2f_i(v/c)$. For example, to accurately measure a 10 cm/sec arterial systolic flow velocity with a 10 MHz probe, the required PRF would be approximately 1.3 KHz. For this reason, linear array systems usually display color-flow Doppler over a limited area of interest within the overall scan.

Linear array systems are significantly more complex than traditional single-element ophthalmic systems. They require sophisticated hardware, firmware, and software to control excitation and echo reception from each transducer element, for beamforming and image display. Thus, these systems have been more costly than simple ophthalmic ultrasound systems. Another impediment towards linear array adoption in ophthalmology is regulatory;

FDA guidelines for diagnostic ultrasound in ophthalmology are more stringent than in any other clinical specialty. For the eye, the regulatory upper limit for mechanical index, (MI, a measure of cavitation risk) is 0.23, whereas it is 1.9 for all other specialties.[49] All commercial ophthalmic ultrasound instruments are by design compliant with the ophthalmic standard. General purpose linear array systems are not, and it is incumbent upon the user to operate the instrument within those guidelines. Doppler modes are especially likely to exceed the ophthalmic limit.[50]

Because of their orientation towards non-ophthalmic clinical specialties (mostly working at lower frequencies than appropriate in ophthalmology), their relatively high cost, and the relatively small user base compared to other specialties, linear array technology has not until recently found its way into ocular imaging other than in neurology (for evaluation of papilledema) and the emergency room. Several manufacturers of general-purpose linear array systems, however, are now offering systems with an FDA-compliant ophthalmic setting. These systems offer synthetic focusing in which subaperture size and focal length vary in tandem to maintain a constant F-number throughout the image, which improves image quality compared to a fixed focus single-element system. Such systems can produce color-flow Doppler images depicting regions where flow is present while in compliance with ophthalmic regulatory requirements. Examples of linear array B-scan and Doppler are provided in Fig 5.

4.3 Plane-wave imaging:

Ultrafast plane-wave imaging can provide Doppler imaging at low acoustic intensity.[51] In this technique, all elements of a linear array transmit together to produce an elongated, unfocused wavefront. Although the transmitted pulse is unfocussed, beamforming can be performed on the received signal using a technique called ‘delay and sum’ in which echo data recorded by each transducer element are brought into phase by triangulating the range from each probe element to each image position and adding appropriate time delays to bring echo data into phase before adding. While computer-intensive, this can now be readily performed in real-time. Because an image can be formed with each transmit, the imaging rate is far faster than that obtainable with a conventionally scanned linear array. In the example of a 100-element array described above, images could be formed at 5 msec intervals, i.e., at 20,000 images/sec. In practice, compound images are formed from several transmits at different angles, which improves resolution and sensitivity, although imaging speed is reduced in proportion to the number of transmits per compound image.

Because the transmitted plane wave is unfocused, acoustic intensity is reduced and color flow and spectral Doppler can be performed within established safety standards. We have performed plane-wave imaging in adults and neonates, acquiring data at 1000–6000 compound scans/sec for 1–3 seconds, allowing capture of several cardiac cycles.[52–54] As each image pixel position is derived from a stack of a thousands of phase-resolved images, Doppler analysis can be performed at any point in the image and spectrograms representing flow velocity over the cardiac cycle produced. Figure 7 illustrates plane-wave color-flow Doppler imaging and spectrograms.

At present, the plane wave technique remains confined to research ultrasound systems and requires greater resources in random access and non-volatile memory as well as central and graphics processor power to store and process the huge amount of data recorded continuously over several seconds for each scan.

4.4 Point-of-care:

At the opposite end of the complexity/cost spectrum are point-of-care (POCUS) ultrasound systems. Ophthalmic POCUS has long existed in the form of handheld pachymeters, e.g., the Accutome PachPen, but portable (e.g., Venue Go, GE Healthcare, Chicago, IL)) and wireless (e.g., Clarius L15 and L20 HD3 systems, Clarius Mobile Health, Vancouver, BC, Canada) linear array-based systems offering B-scan have recently become available with display on devices such as a smartphone or tablet. While not specifically designed for imaging the eye, they economically address the need for ocular imaging especially in pediatrics, neurology, and emergency medicine where dedicated ophthalmic scanners may be unavailable.

5. Conclusion

From submarine warfare to medical imaging, ultrasound has allowed visualization of the invisible. Just as lives depended upon detection of the unseen enemy during war, lives and quality-of-life now depend upon the capabilities of diagnostic ultrasound imaging systems.

While the physics of reflection, refraction, attenuation, and scattering are eternal, ophthalmic ultrasound systems have evolved from the rudimentary devices devised in the aftermath of WW2 to the digital systems of today. The technologies of transducer design and fabrication, of ultrasound signal processing, ultrafast imaging and Doppler methods continue to undergo development. The author has witnessed this progression over his professional life and rather than slowing, the pace of change is accelerating. But whatever technological changes the future may bring, appreciation of the physical principles of ultrasound in the context of ocular anatomy and pathology will be incumbent upon the practitioner to effectively apply technologic advances.

6. Expert opinion

Many of the advances described above relate to the introduction of array-based transducers. The annular array may be regarded as a distinct, but nevertheless, incremental improvement over the traditional ophthalmic fixed focus, single element probe. Annular arrays can provide an appropriate focal length for specific diagnostic situations and improved depth of field. In addition, they provide an axially symmetric beamform, which is not the case for linear arrays. Their chief shortcoming is the necessity of mechanical scanning, which severely limits scan rate.

Linear arrays benefit from 50 years of development in specialties other than the eye. In addition to B-scan imaging of structure, they offer Doppler imaging and measurement of blood flow velocity as well as suites of other processing modes such as tissue harmonic imaging and elastography. While some general-purpose linear array systems now offer an ophthalmology mode compliant with regulatory guidelines, the mode may be limited in

terms of which probes and which techniques can be utilized in order to maintain compliance. Furthermore, general purpose instruments will not include ophthalmology-specific analysis and reporting modes (e.g., for axial length determination and IOL power calculations). Although linear arrays in the UBM frequency range are available in preclinical research systems (e.g., the Vevo F2, FUJIFILM VisualSonics, Inc., Toronto, ON, Canada), this remains unavailable in current commercial clinical instruments.

Given the advantages of linear arrays over mechanically scanned systems, it is probable that this technology will gradually supplant our current mechanical B-scan technology. This is true given the advantages in image quality, new (to ophthalmology) imaging modalities, miniaturization, and their substantial decline in cost, which is now comparable to high-end mechanical ophthalmic systems. As array technology is adapted to ophthalmology, application-specific biometric analysis and reporting modes will without doubt be offered. It is also probable that array based UBM systems will appear.

In the more distant future, even more advanced technology based on two-dimensional matrix arrays will arrive, offering 3D and 4D (3D + time) imaging without moving parts.[55] One can anticipate systems offering acquisition of thousands of volumes per second, enabling evaluation of ocular structure and blood flow, and improved assessment of the vasculature and space occupying lesions. Thus, while ultrasound is a ‘mature’ technology, it is a mistake to believe that it is static – the best is yet to come.

Funding

This paper was funded by NIH grants R01 EY025215, R01 EB032082, P30 EY019007 and an unrestricted grant to the Columbia University Department of Ophthalmology from Research to Prevent Blindness.

References

1. Silverman RH, Vinarsky E, Woods SM, Lizzi FL, Coleman DJ. The effect of transducer bandwidth on ultrasonic image characteristics. Retina, 15(1), 37–42 (1995). [PubMed: 7754247]
2. Oksala A, Lehtinen A. [Diagnostic value of ultrasonics in ophthalmology]. Ophthalmologica, 134(6), 387–395 (1957). [PubMed: 13493993]
3. Baum G, Greenwood I. The application of ultrasonics locating techniques to ophthalmology; theoretic considerations and acoustic properties of ocular media. I. Reflective properties. Am J Ophthalmol, 46(5 Pt 2), 319–329 (1958). [PubMed: 13595080]
4. Baum G, Greenwood I. The application of ultrasonic locating techniques to ophthalmology. II. Ultrasonic slit lamp in the ultrasonic visualization of soft tissues. AMA Arch Ophthalmol, 60(2), 263–279 (1958). [PubMed: 13558798]
5. Jansson F, Kock E. Determination of the velocity of ultrasound in the human lens and vitreous. Acta Ophthalmol (Copenh), 40, 420–433 (1962). [PubMed: 13957440]
6. Begui ZE. Acoustic Properties of the Refractive Media of the Eye. The Journal of the Acoustical Society of America, 26(3), 365–368 (2005).
7. Oksala A, Lehtinen A. Measurement of the velocity of sound in some parts of the eye. Acta Ophthalmol (Copenh), 36(4), 633–639 (1958). [PubMed: 13594375]
8. Linebarger EJ, Hardten DR, Shah GK, Lindstrom RL. Phacoemulsification and modern cataract surgery. Surv Ophthalmol, 44(2), 123–147 (1999). [PubMed: 10541151]
9. Apple DJ. Sir Harold Ridley and His Fight for Sight: He Changed the World So That We May Better See It (SLACK, Inc., Thorofare, NJ, 2006).

10. Coleman DJ, Carlin B. A New System for Visual Axis Measurements in the Human Eye Using Ultrasound. Archives of Ophthalmology, 77(1), 124–127 (1967). [PubMed: 6015709]
11. Hennessy MP, Franzco, Chan DG. Contact versus immersion biometry of axial length before cataract surgery. J Cataract Refract Surg, 29(11), 2195–2198 (2003). [PubMed: 14670431]
12. Olsen T, Nielsen PJ. Immersion versus contact technique in the measurement of axial length by ultrasound. Acta Ophthalmol (Copenh), 67(1), 101–102 (1989). [PubMed: 2672694]
13. Holladay JT, Musgrove KH, Prager TC, Lewis JW, Chandler TY, Ruiz RS. A three-part system for refining intraocular lens power calculations. Journal of Cataract & Refractive Surgery, 14(1), 17–24 (1988). [PubMed: 3339543]
14. Hoffer KJ. The Hoffer Q formula: A comparison of theoretic and regression formulas. Journal of Cataract & Refractive Surgery, 19(6), 700–712 (1993). [PubMed: 8271165]
15. Retzlaff JA, Sanders DR, Kraff MC. Development of the SRK/T intraocular lens implant power calculation formula. Journal of Cataract & Refractive Surgery, 16(3), 333–340 (1990). [PubMed: 2355321]
16. Baxter J, Atwan N. A Comparison Between Ultrasound Pachymetry and CASIA2 (Anterior-Segment Optical Coherence Tomography) in the Measurement of Central Corneal Thickness. Cureus, 15(6), e39921 (2023). [PubMed: 37409208]
17. Doğan M, Ertan E. Comparison of central corneal thickness measurements with standard ultrasonic pachymetry and optical devices. Clin Exp Optom, 102(2), 126–130 (2019). [PubMed: 30557910]
18. Williams R, Fink BA, King-Smith PE, Mitchell GL. Central corneal thickness measurements: using an ultrasonic instrument and 4 optical instruments. Cornea, 30(11), 1238–1243 (2011). [PubMed: 21926567]
19. Coleman DJ, Konig WF, Katz L. A hand-operated, ultrasound scan system for ophthalmic evaluation. Am J Ophthalmol, 68(2), 256–263 (1969). [PubMed: 4307960]
20. Coleman DJ, Dallow RL, Smith ME. Immersion ultrasonography: simultaneous A-scan and B-scan. Int Ophthalmol Clin, 19(4), 67–102 (1979). [PubMed: 536137]
21. Bronson NR. Development of a simple B-scan ultrasonoscope. Trans Am Ophthalmol Soc, 70, 365–408 (1972). [PubMed: 4663678]
22. Sherar MD, Foster FS. The design and fabrication of high frequency poly(vinylidene fluoride) transducers. Ultrason Imaging, 11(2), 75–94 (1989). [PubMed: 2734975]
23. Sherar MD, Starkoski BG, Taylor WB, Foster FS. A 100 MHz B-scan ultrasound backscatter microscope. Ultrason Imaging, 11(2), 95–105 (1989). [PubMed: 2660392]
24. Pavlin CJ, Harasiewicz K, Sherar MD, Foster FS. Clinical use of ultrasound biomicroscopy. Ophthalmology, 98(3), 287–295 (1991). [PubMed: 2023747]
25. Silverman RH, Reinstein DZ, Raevsky T, Coleman DJ. Improved system for sonographic imaging and biometry of the cornea. J Ultrasound Med, 16(2), 117–124 (1997). [PubMed: 9166804]
26. Reinstein DZ, Silverman RH, Raevsky T et al. Arc-scanning very high-frequency digital ultrasound for 3D pachymetric mapping of the corneal epithelium and stroma in laser in situ keratomileusis. J Refract Surg, 16(4), 414–430 (2000). [PubMed: 10939721]
27. Reinstein DZ, Archer TJ, Urs R, Gobbe M, RoyChoudhury A, Silverman RH. Detection of Keratoconus in Clinically and Algorithmically Topographically Normal Fellow Eyes Using Epithelial Thickness Analysis. J Refract Surg, 31(11), 736–744 (2015). [PubMed: 26544561]
28. Reinstein DZ, Gobbe M, Archer TJ, Silverman RH, Coleman DJ. Epithelial, stromal, and total corneal thickness in keratoconus: three-dimensional display with artemis very-high frequency digital ultrasound. J Refract Surg, 26(4), 259–271 (2010). [PubMed: 20415322]
29. Silverman RH, Urs R, Roychoudhury A, Archer TJ, Gobbe M, Reinstein DZ. Epithelial remodeling as basis for machine-based identification of keratoconus. Invest Ophthalmol Vis Sci, 55(3), 1580–1587 (2014). [PubMed: 24557351]
30. Reinstein DZ, Archer TJ, Gobbe M. LASIK flap thickness profile and reproducibility of the standard vs zero compression Hansatome microkeratomes: three-dimensional display with Artemis VHF digital ultrasound. J Refract Surg, 27(6), 417–426 (2011). [PubMed: 21410084]
31. Reinstein DZ, Archer TJ, Gobbe M, Johnson N. Accuracy and reproducibility of artemis central flap thickness and visual outcomes of LASIK with the Carl Zeiss Meditec VisuMax femtosecond

laser and MEL 80 excimer laser platforms. J Refract Surg, 26(2), 107–119 (2010). [PubMed: 20163075]

32. Reinstein DZ, Sutton HF, Srivannaboon S, Silverman RH, Archer TJ, Coleman DJ. Evaluating microkeratome efficacy by 3D corneal lamellar flap thickness accuracy and reproducibility using Artemis VHF digital ultrasound arc-scanning. J Refract Surg, 22(5), 431–440 (2006). [PubMed: 16722480]
33. Ang M, Baskaran M, Werkmeister RM et al. Anterior segment optical coherence tomography. Prog Retin Eye Res, 66, 132–156 (2018). [PubMed: 29635068]
34. Vira J, Marchese A, Singh RB, Agarwal A. Swept-source optical coherence tomography imaging of the retinochoroid and beyond. Expert Rev Med Devices, 17(5), 413–426 (2020). [PubMed: 32275451]
35. Spaide RF, Koizumi H, Pozzoni MC. Enhanced depth imaging spectral-domain optical coherence tomography. Am J Ophthalmol, 146(4), 496–500 (2008). [PubMed: 18639219]
36. Mrejen S, Spaide RF. Optical coherence tomography: imaging of the choroid and beyond. Surv Ophthalmol, 58(5), 387–429 (2013). [PubMed: 23916620]
37. Ursea R, Feng M, Urs R, RoyChoudhury A, Silverman RH. Comparison of artemis 2 ultrasound and Visante optical coherence tomography corneal thickness profiles. J Refract Surg, 29(1), 36–41 (2013). [PubMed: 23205905]
38. Wevers M, Strabbing EM, Engin O, Gardeniers M, Koudstaal MJ. CT parameters in pure orbital wall fractures and their relevance in the choice of treatment and patient outcome: a systematic review. Int J Oral Maxillofac Surg, 51(6), 782–789 (2022). [PubMed: 34696942]
39. Brenner D, Elliston C, Hall E, Berdon W. Estimated risks of radiation-induced fatal cancer from pediatric CT. AJR Am J Roentgenol, 176(2), 289–296 (2001). [PubMed: 11159059]
40. Poon R, Badawy MK. Radiation dose and risk to the lens of the eye during CT examinations of the brain. J Med Imaging Radiat Oncol, 63(6), 786–794 (2019). [PubMed: 31520467]
41. Griffin AS, Hoang JK, Malinzak MD. CT and MRI of the Orbit. Int Ophthalmol Clin, 58(2), 25–59 (2018).
42. Berger A Magnetic resonance imaging. Bmj, 324(7328), 35 (2002). [PubMed: 11777806]
43. Lindner T, Langner S, Graessl A et al. High spatial resolution in vivo magnetic resonance imaging of the human eye, orbit, nervus opticus and optic nerve sheath at 7.0 Tesla. Exp Eye Res, 125, 89–94 (2014). [PubMed: 24928314]
44. Glarin RK, Nguyen BN, Cleary JO et al. MR-EYE: High-Resolution MRI of the Human Eye and Orbit at Ultrahigh Field (7T). Magn Reson Imaging Clin N Am, 29(1), 103–116 (2021). [PubMed: 33237011]
45. Steinborn M, Fiegler J, Kraus V et al. High resolution ultrasound and magnetic resonance imaging of the optic nerve and the optic nerve sheath: anatomic correlation and clinical importance. Ultraschall Med, 32(6), 608–613 (2011). [PubMed: 21058238]
46. Silverman RH, Ketterling JA, Coleman DJ. High-frequency ultrasonic imaging of the anterior segment using an annular array transducer. Ophthalmology, 114(4), 816–822 (2007). [PubMed: 17141314]
47. Silverman RH, Ketterling JA, Mamou J, Lloyd HO, Filoux E, Coleman DJ. Pulse-encoded ultrasound imaging of the vitreous with an annular array. Ophthalmic Surg Lasers Imaging, 43(1), 82–86 (2012). [PubMed: 21902166]
48. Hedrick WR, Hykes DL. Beam Steering and Focusing With Linear Phiased Arrays. Journal of Diagnostic Medical Sonography, 12(5), 211–215 (1996).
49. Food and Drug Administration. Marketing Clearance of Diagnostic Ultrasound Systems and Transducers, Guidance for Industry and Food and Drug Administration Staff (2019).
50. Abramowicz JS, Adhikari S, Dickman E et al. Ocular Ultrasound: Review of Bioeffects and Safety, Including Fetal and Point of Care Perspective: Review of Bioeffects and Safety, Including Fetal and Point-of-Care Perspective. J Ultrasound Med, 41(7), 1609–1622 (2022). [PubMed: 34724263]
51. Tanter M, Fink M. Ultrafast imaging in biomedical ultrasound. IEEE transactions on ultrasonics, ferroelectrics, and frequency control, 61(1), 102–119 (2014). [PubMed: 24402899]
52. Urs R, Ketterling JA, Silverman RH. Ultrafast ultrasound imaging of ocular anatomy and blood flow. Invest Ophthalmol Vis Sci, 57(8), 3810–3816 (2016). [PubMed: 27428169]

53. Urs R, Ketterling JA, Yu ACH, Lloyd HO, Yiu BYS, Silverman RH. Ultrasound Imaging and Measurement of Choroidal Blood Flow. Transl Vis Sci Technol, 7(5), 5 (2018).

54. Silverman RH, Urs R, Wapner RJ, Bearelly S. Plane-Wave Ultrasound Doppler of the Eye in Preeclampsia. Transl Vis Sci Technol, 9(10), 14 (2020).

55. Correia M, Provost J, Tanter M, Pernot M. 4D ultrafast ultrasound flow imaging: in vivo quantification of arterial volumetric flow rate in a single heartbeat. Phys Med Biol, 61(23), L48–l61 (2016). [PubMed: 27811406]

Article highlights:

- Medical diagnostic ultrasound developed in the aftermath of the second world war as a spinoff of Sonar technology used for underwater range finding.
- While ophthalmic ultrasound has largely been based on mechanically scanned, focused single-element transducer technology, virtually all other clinical specialties use linear array-based systems.
- Array-based systems allow control of focal depth. Linear arrays offer high scan rates and can provide Doppler to visualize and measure blood-flow.
- The advantages and decreasing cost of linear array systems is leading towards greater utilization for ophthalmic imaging.
- While the principles of ultrasound imaging are unchanged, the technology, especially in array-based systems, continues to advance.

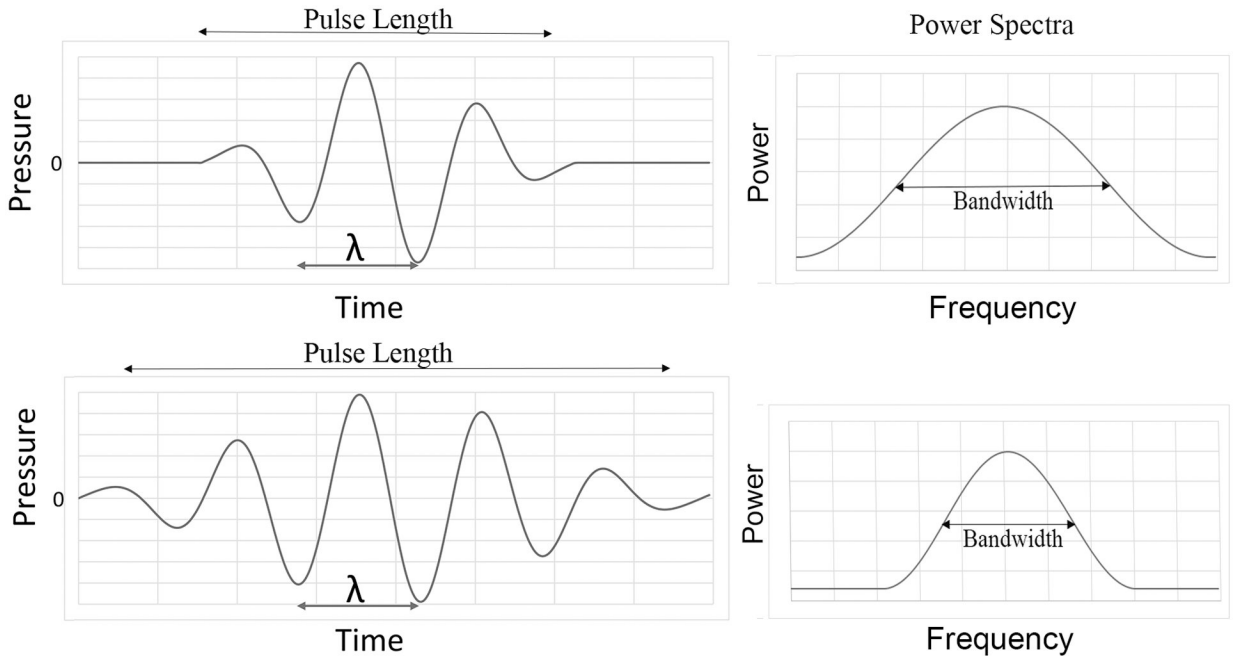

Figure 1:

Left: Plots representing ultrasound waveform of a highly damped (top) and a poorly damped (bottom) transducer of the same wavelength (λ). To the right of each plot is the power spectrum corresponding to each waveform. Bandwidth (usually measured at 50% of maximum spectral power) is inversely related to pulse-length.

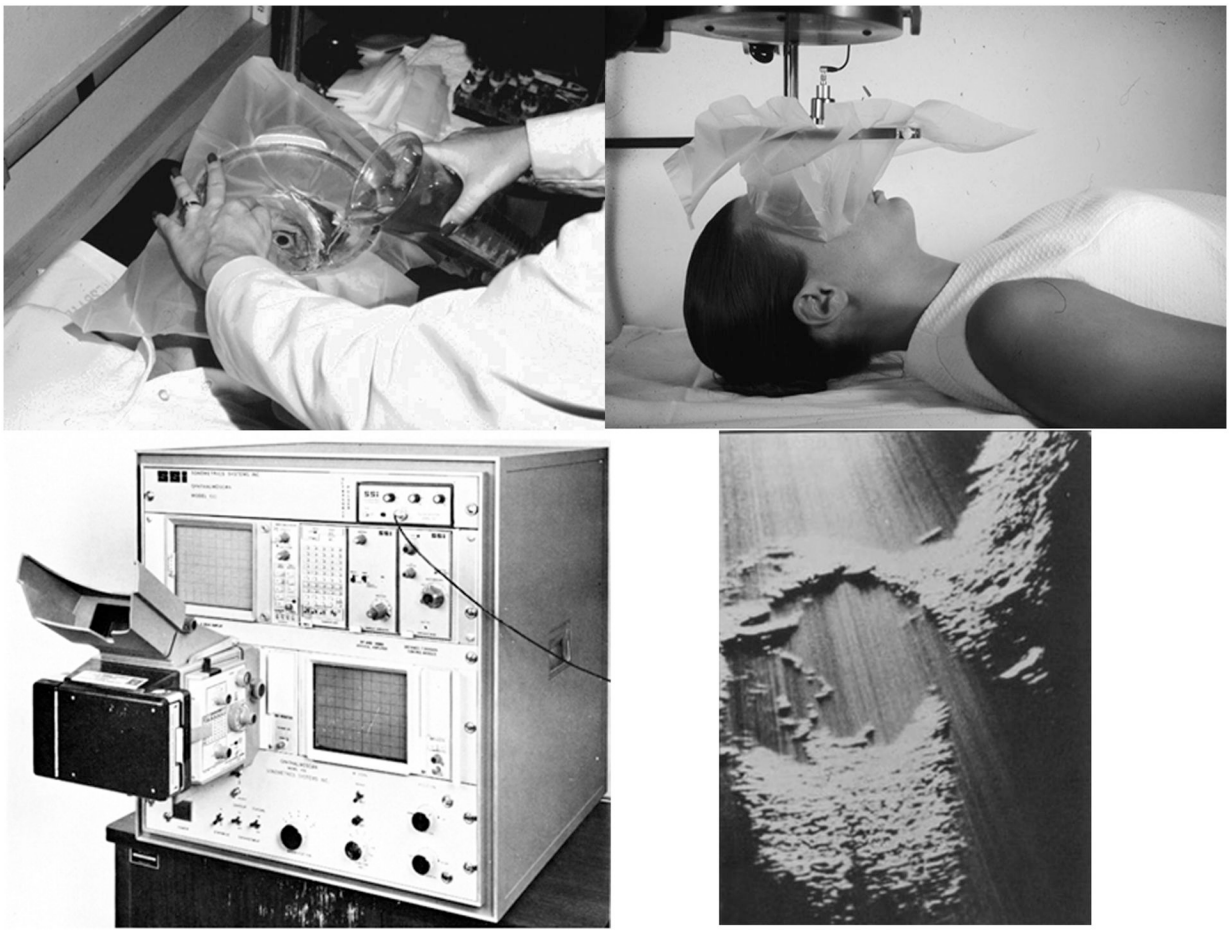

Figure 2:
1970's setup for immersion ultrasonography. The probe was pivoted by hand to sweep out a B-scan or held steady for an A-scan while the shutter of the polaroid camera facing the display was held open. Analog images had limited dynamic range, but resolution was excellent. The immersion technique was particularly good for visualizing the anterior segment since the probe could be positioned far enough away to place its focus where needed.

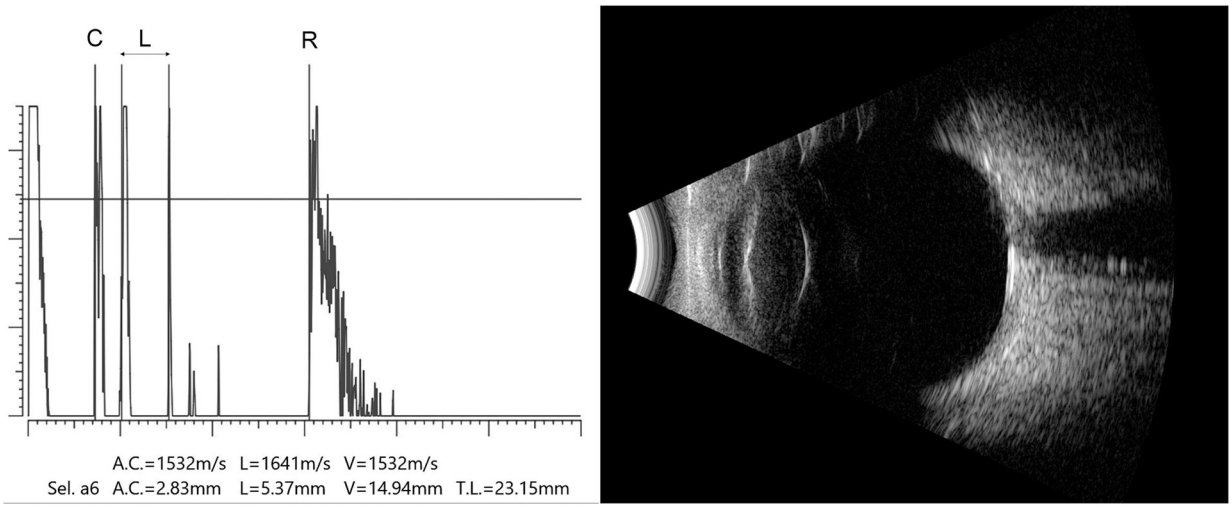

Figure 3:

Biometric immersion A-scan and contact axial B-scan images of 73-year-old subject. Note faint echoes in mid vitreous in the A-scan due to floaters. Lens does not show internal echoes indicative of cataract. C=corneal, L=lens, R=retina.

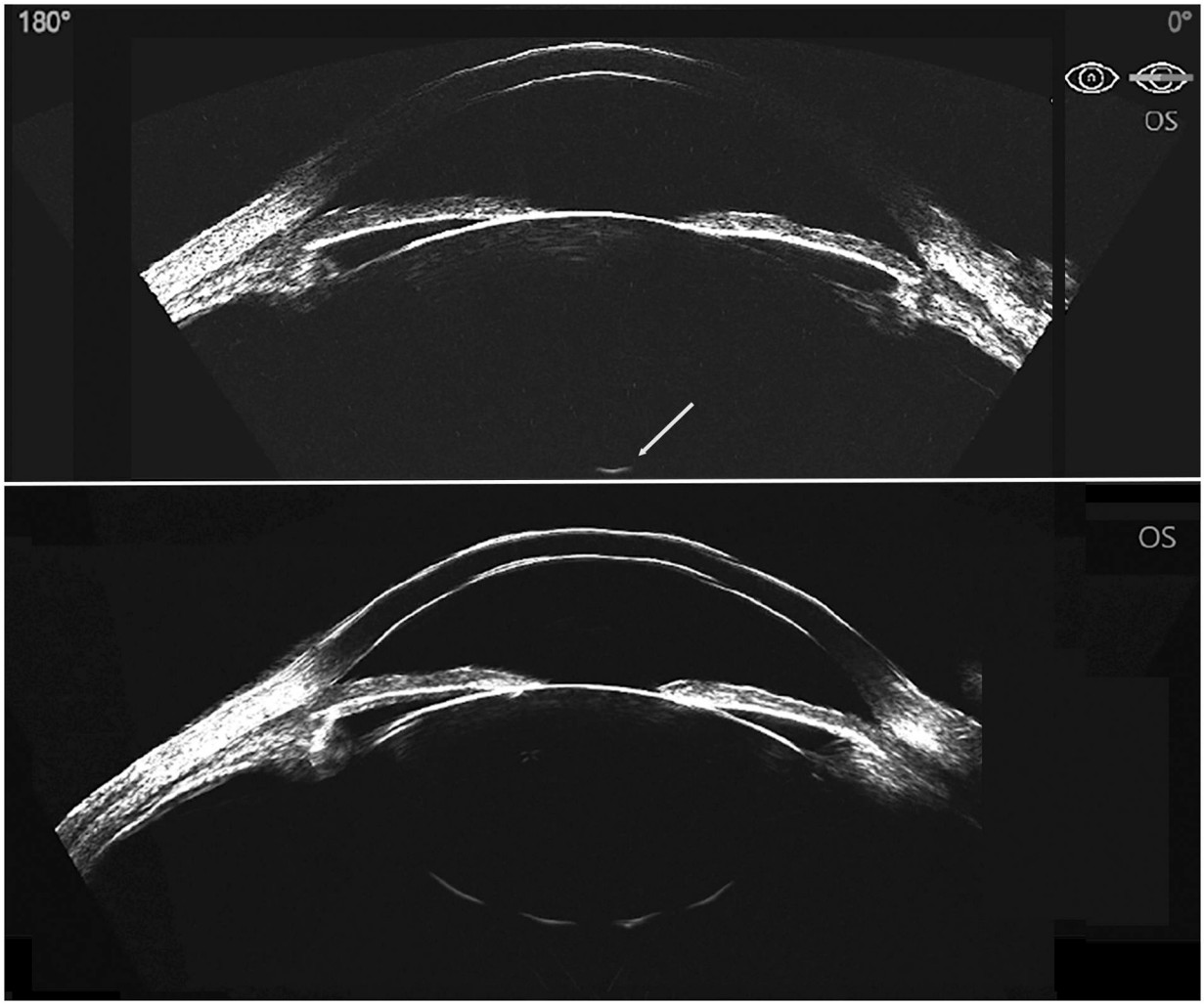

Figure 4:
UBM images of anterior segment obtained by shallow arc scan (top) match to curvature of eye and by compounding of multiple arc and linear scans (bottom) on the Insight system. Due to specular reflectivity of lens capsule, the posterior capsule is only seen at the posterior pole in the arc scan (arrow) versus nearly full outline in compound image.

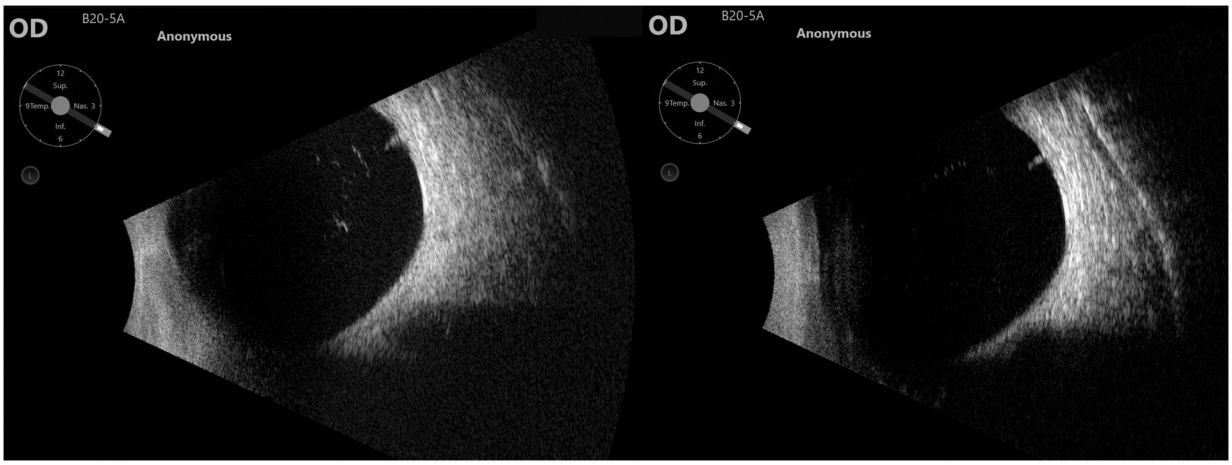

Figure 5:

20 MHz B-scan images obtained with Quantel Absolu annular array in vitreous (left) and retina (right) mode settings. The images show a lesion supero-temporally at the site of laser-treated retinal tear that occurred following posterior vitreous detachment 12 years previously. Note greater detail in depiction of vitreous debris in vitreous-mode image and improved depiction of retina and orbital tissues in retina-mode.

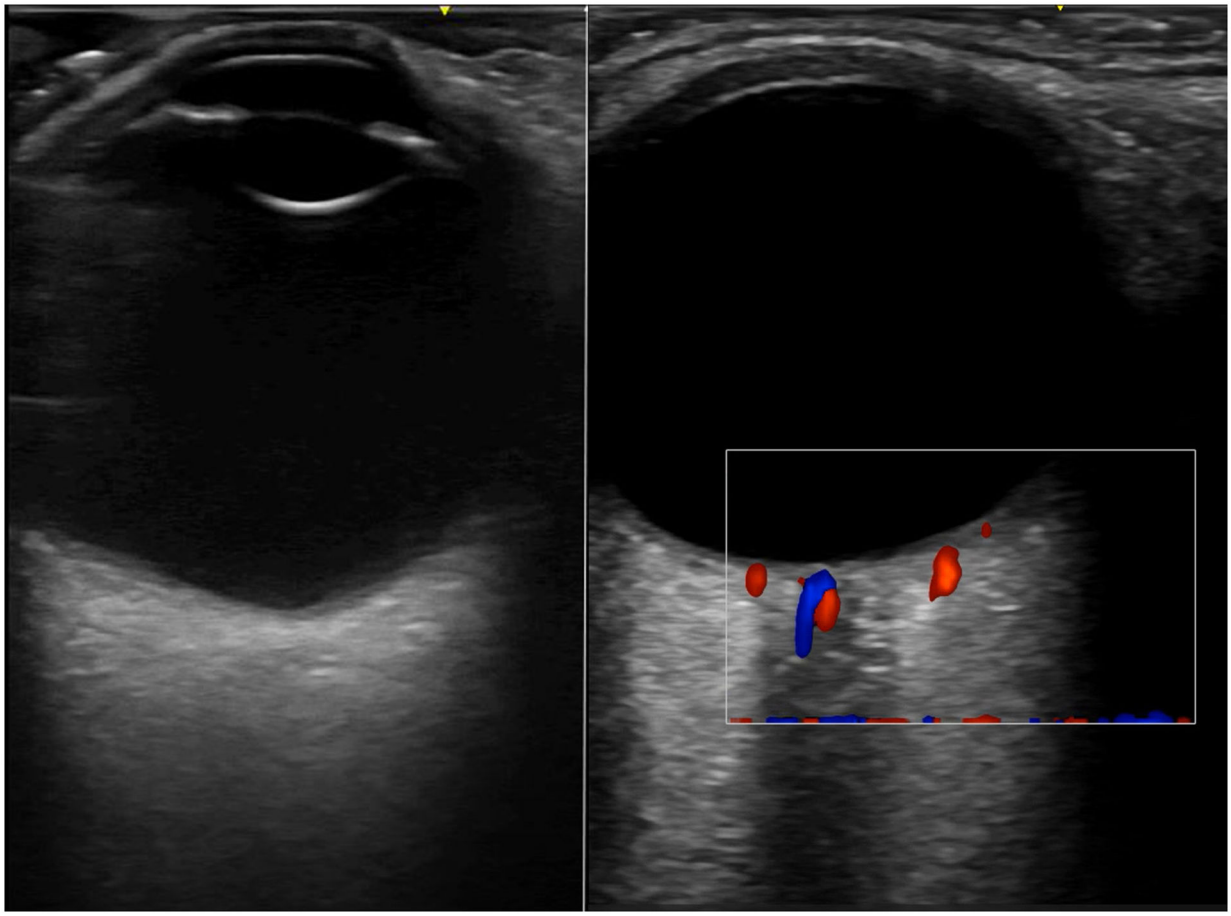

Figure 6:
Axial B-scan and color-flow Doppler image obtained on GE Venue Go ultrasound system with L4–20t-RS linear array probe. The central retinal artery (red) and vein (blue) are visualized.

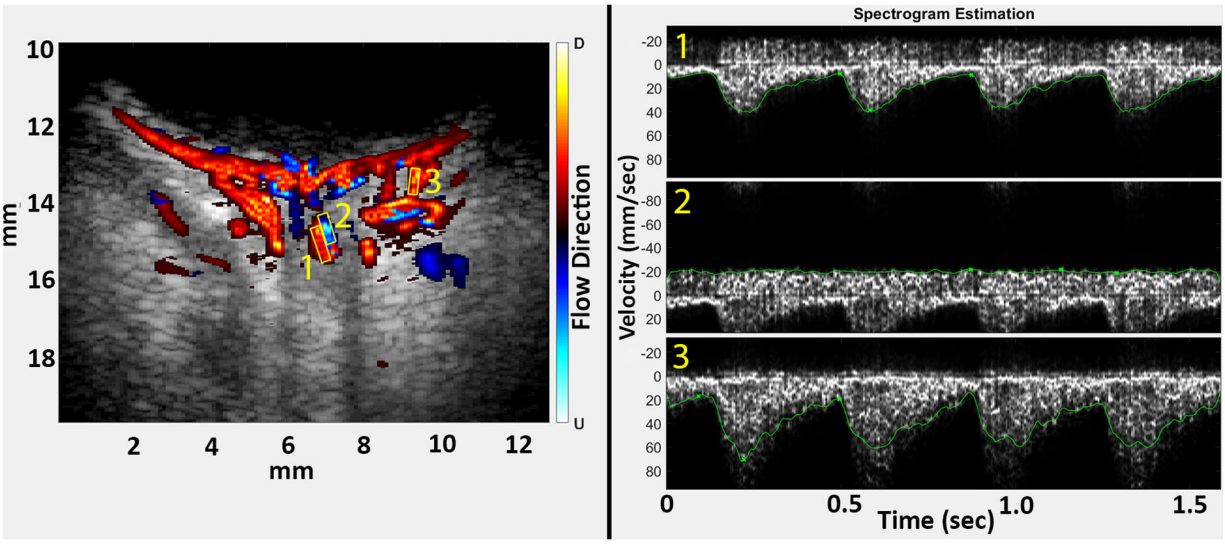

Figure 7:

Plane-wave Doppler color flow image and spectrograms of pre-term, low birthweight neonate evaluated at cribside in neonatal intensive care unit. Data were acquired from 6 compounded angled transmits with 3000 compound images acquired per second. Spectrograms depict flow velocity over 1.5 seconds in the central retinal artery (1), central retinal vein (2) and short posterior ciliary artery (3).

Table 1.

Ultrasound and OCT imaging modes. Frequency, wavelength and acquisition rates vary with manufacturer, but these are typical. Note that some research OCT systems can now acquire A-scan lines at 1 MHz or more.

Technology	Method	Application	Frequency (MHz)	Hz
Ultrasound	A-scan	Axial length	10	50–100
		Corneal pachymetry	20–50	
	B-scan	Eye and orbit	10–20	10–20
	UBM	Anterior segment, retro-iridal space, ciliary body	35–50	8–20
	Linear array	Eye and orbit	8–20	>100
	Plane wave	Eye and orbit, blood flow	8–20	≤20,000
OCT			**Wavelength (nm)**	**A-scan/sec (kHz)**
	Anterior segment	Cornea, iris, angle	850, 1050, 1300	50–200
	Posterior	Vitreous, retina, choroid, optic nerve	850, 1050	
	Angiography	Retinal, choroidal vasculature		